PROCEEDINGS OF SCIENCE

Second Knee in Cosmic Ray Spectrum at Energy $\sim 10^{17}$ eV by Yakutsk Data

Stanislav Knurenko∗†
Yu. G. Shafer Institute of Cosmophysical Research and Aeronomy
E-mail: knurenko@ikfia.ysn.ru

Igor Petrov
Yu. G. Shafer Institute of Cosmophysical Research and Aeronomy
E-mail: igor.petrov@ikfia.ysn.ru

The paper presents cosmic ray spectrum by Small Cherenkov Yakutsk array data for 20 continuous years of observation. The spectrum is obtained from Cherenkov light flux - the energy scattered by charged particles of air showers in the atmosphere. It has been shown by measurements that in the cosmic ray spectrum there is a break in the slope at energy $\sim 10^{17}$ eV. The reliability of the result is based on spectra of other compact array experiments and simulations to check for systematic uncertainties, which could affect the shape of the spectrum. Another confirmation is change in mass composition of cosmic ray obtained from longitudinal development of air showers in energy region 10^{16}-10^{18} eV.

36th International Cosmic Ray Conference -ICRC2019-
July 24th - August 1st, 2019
Madison, WI, U.S.A.

∗Speaker.
†A footnote may follow.

PoS(ICRC2019)384

1. Introduction

The main objectives of ultra-high energy cosmic ray (CR) studies are to determine the anisotropy, energy spectrum, and chemical composition of primary CR particles. These characteristics of cosmic rays play an important role in understanding the origin, acceleration, and propagation of primary particles of different energies. In the energy range of 10^{12}-10^{14} eV, such measurements are performed on satellites [1, 2, 3] and by launching balloons to altitudes of 35 km [4, 5]. In these experiments, it is possible to directly measure both the chemical composition of the particles and their elemental spectra. The only drawback of such experiments is the small area of the lifted detectors and the limited observation time. At energies above 10^{14} eV due to low intensity cosmic rays can be studied only by extensive air showers (EAS), i.e. indirectly, by tracking the cascade processes in the atmosphere and detecting the charged particles fluxes, muons, ionization luminescence, and Cherenkov light of air showers at sea level. Due to the very wide spectrum of cosmic rays, arrays with variety of sizes are employed: compact ones with an area of s < 1 km^2 that register air showers up to energies of 10^{18} eV, average sized arrays with s < 20 km^2 that register up to energies of 10^{19} eV and huge arrays such as Auger [6], Telescope Array [7] for higher energies.

2. Small Cherenkov Array

In 1994, a Small Cherenkov array was created within the central part of the Yakutsk array to register EAS of moderate energies (Fig. 1). One distinctive feature of the Small Cherenkov is that it measures several components of EAS like muons, electrons, and Cherenkov radiation, unlike other compact arrays like KASCADE [8] or TUNKA [9]. This allows a broader look at the development of the shower, including longitudinal development, registering the spatial distribution of electrons, muons, and EAS Cherenkov light, at sea level [10, 11] and its longitudinal profile using the measurement of the flux of Cherenkov photons (which are generated throughout development of the shower in the atmosphere) by integral and differential Cherenkov detectors [11, 12].

3. Air shower measurements simulation at the Small Cherenkov Array

To estimate the precision of determining air shower characteristics at the Yakutsk array, a full Monte Carlo simulation was carried out. The simulation results are shown in Table 1.

E_0	σ(R)	σN_s	σ(Q(100))	σ(Q(200))	σ(Q(400))	$\sigma(\rho_s(300))$	$\sigma(\rho_s(600))$	$\sigma(\theta)$
2	9.7	0.15	0.17	-	-	-	-	1.3
10	7.2	0.11	0.15	-	-	-	-	1.0
100	15.5	0.27	0.15	0.25	-	-	-	5.7
200	34.6	0.32	0.20	0.20	0.22	0.25	-	5.4
1000	26.7	0.35	-	-	0.20	0.17	0.19	3.3

In Table 1: σ(R) - axis reconstruction error [m]; δN_s - total number of charged particles determination error, σ(Q(100)), σ(Q(200)) and σ(Q(400)) - errors of determining the classification parameters of the Cherenkov radiation flux at a distance 100, 200 and 400 m respectively; $\sigma(\rho_s(300))$ and $\sigma(\rho_s(600))$ - errors of determining of total charged particle flux density at 300 and 600 m respectively; $\sigma(\theta)$ - zenith angle determination uncertainty.

PoS(ICRC2019)384

In a real atmosphere, there is always a noticeable contribution of light loss on aerosol particles of different sizes. In addition, uncertainty is also caused by the extreme continental climate in the array region, i.e. in winter a non-standard atmosphere is formed above the array, with parameters that differ significantly from the atmosphere during the summer period. As it was shown in [13, 14] in winter, with near-ground mists and haze, the maximum flux attenuation of Cherenkov light at distances of 100-400 m from the shower axis reaches ∼ (30-40)%, while under excellent weather conditions the losses do not exceed 10%, which occurs due to Rayleigh scattering of the light in the atmosphere. Because of this, constant observations of the atmosphere are conducted at the Yakutsk array during optical observation periods [14] and the obtained data on the atmospheric transparency are taken into account when determining certain characteristics of air showers, in particular, energy and depth of maximum development of the EAS [15].

The simulation algorithm also included triggers: taking into account the threshold of detectors and their fluctuations in the conditions of background illumination when measuring the flux of Cherenkov light. At the Yakutsk array, shower events are registered when one of two triggers is present: a trigger from the Cherenkov detectors of the Small Cherenkov array that registers showers with an energy of 10^{15}-10^{17} eV; a second trigger is from a large array of scintillation detectors, which is triggered by the arrival of showers with energy above 10^{17} eV.

Since different triggers select events of air showers with different energies, the transition effect should affect the transition from one trigger to another. At the energy boundary, the effective collection area of showers will vary. For large showers, it is underestimated, and for small showers, on the contrary, it is overestimated. With correction of the effective area for events with high-energy showers, this effect was reduced to 15% [16].

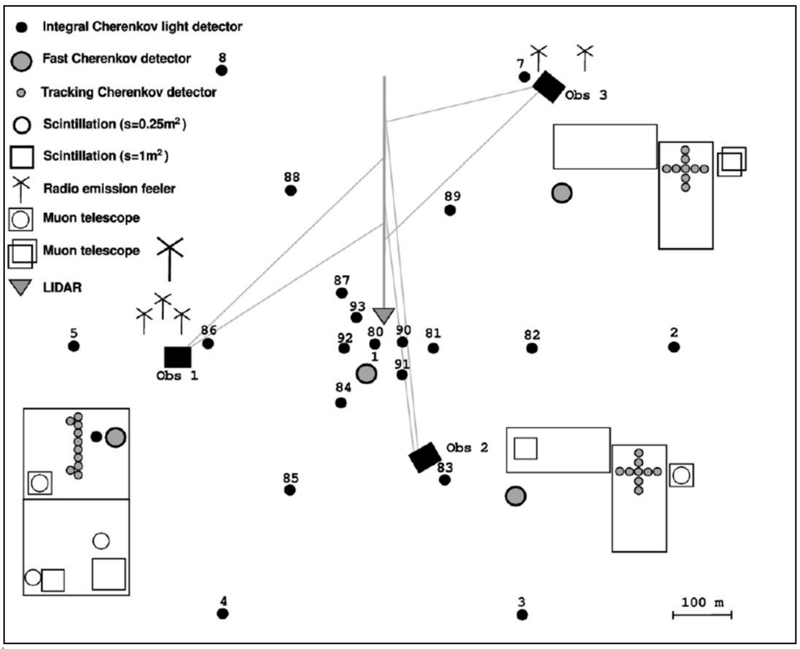

Figure 1: The layout of the detectors of charged particles, muons, and Cherenkov light on the Small Cherenkov array located in the center of the Yakutsk array

4. Air shower energy estimation

For showers with an energy < 500 PeV, the total number of charged particles at sea level is calculated with an accuracy of 10-25% and total flux of Cherenkov light with 10-15% accuracy. It allows one to obtain the necessary information about measured parameters of air showers, which are necessary for energy estimation by a calorimetry method using all EAS components observed at the array: electrons, muons, and the total Cherenkov light flux.

The data were obtained at the Small Cherenkov array for a long period starting from 1994 to 2014. Later the data was averaged in narrow intervals of energy and zenith angles.

At the Yakutsk array, the primary energy of the particle that produced the air shower is determined by the energy balance method:

$$E_0 = E_{ei} + E_{el} + E_\mu + E_{hi} + E_{\mu i} + E_\nu \quad (4.1)$$

Where E_{ei} - the energy scattered by electrons in the atmosphere, E_{el} - the energy carried by electrons below level of observation, E_μ - muon component energy, E_{hi} - ionization losses of hadrons in the atmosphere, $E_{\mu i}$ - ionization losses of muons in the atmosphere, E_ν - the energy of neutrinos.

The parameters of the formula (1) were determined empirically, for energies in the range $5\cdot10^{15}$-$3\cdot10^{17}$ eV [16]

The parameters Q (100), Q(200), and Q (400) weakly depend on the zenith angle. This means that the energy estimation by these parameters has less uncertainty. To determine the shower energy by these parameters, we used formulas derived empirically:

$$E_0 = (5.75 \pm 1.39) \cdot 10^{16} \cdot (Q(100)/10^7)^{0.86\pm0.03} \quad (4.2)$$

$$E_0 = (1.78 \pm 0.44) \cdot 10^{17} \cdot (Q(200)/10^7)^{1.01\pm0.04} \quad (4.3)$$

$$E_0 = (8.91 \pm 1.96) \cdot 10^{17} \cdot (Q(400)/10^7)^{1.03\pm0.05} \quad (4.4)$$

where Q(100),Q(200), and Q(400) - Cherenkov light flux density at the distances 100, 200, and 400 m respectively.

Fig. 3 shows the dependence of E_{em} / E_0 on energy. The parameter $E_{em} = E_{ei} + E_{el}$ was determined by the formula (5) and (6) [16]. Where E_{em} is the energy transferred to the electromagnetic component, E_{ei} is the energy scattered by electrons in the atmosphere above the observation level, Eel is the energy carried by electrons below level of observation. In Fig. 3, the experimental data of the Yakutsk array are compared with the calculations of QGSJetII-03 [17] taken from [18].

$$E_{ei} = k(x, P_\lambda) \cdot \Phi \quad (4.5)$$

Where Φ is the total flux of Cherenkov light; k (x, P_λ) is the approximation coefficient (calculated value), taking into account the transparency of the real atmosphere, the nature of the longitudinal development of the shower (energy spectrum of secondary particles and its dependence on

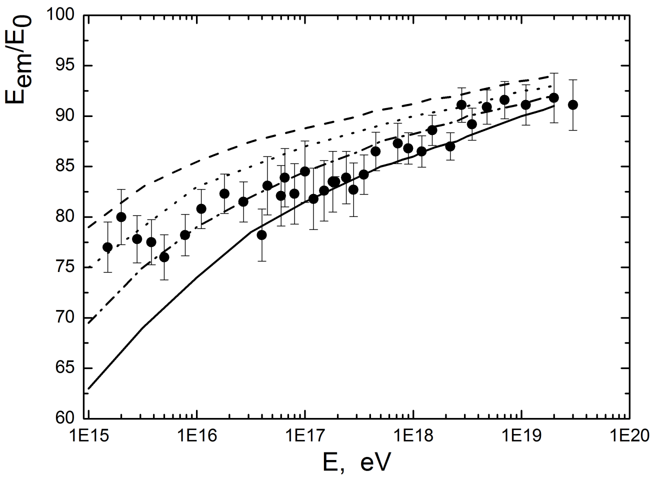

Figure 2: The fraction of energy transferred to the electromagnetic component according to the registration of Cherenkov light of EAS at the Yakutsk array and the QGSJetII-03 model of hadron interactions for the proton p (dash), helium He (dots), CNO nuclei (dash-dot) and iron Fe nucleus (solid).

the age of the shower) and expressed through the depth of the maximum of EAS X_{max}, measured at the array.

$$E_{el} = 2.2 \cdot 10^6 \cdot N_s(X_0) \cdot \lambda_{eff} \tag{4.6}$$

where N_s (X_0) is the total number of charged particles at sea level, and λ_{eff} is the absorption range of the shower particles, found from the correlation of the parameters Ns (X_0) and Q (400) at different zenith angles [16].

As can be seen from Fig. 2, on average, the experimental data are consistent with calculations based on the QGSjet-03 model of hadron interactions and the mixed composition of primary particles.

5. Energy Spectrum of Air Showers

Using the database of the Small Cherenkov array for the period from 1994 to 2014 and applying the criteria described above, we estimated the intensity of EAS events registered in a given interval in terms of the energy ΔE_i and the zenith angle $\Delta\theta_i$ per unit of the effective area of the array. The resulting spectrum is shown in Fig. 3a.

As can be seen from Fig. 3a, the obtained spectrum has two features at the energy $\sim 3\cdot 10^{15}$ eV (first knee) and at the energy $\sim 10^{17}$ eV (second knee). The first knee is characterized by the slope γ_1 = 2.70±0.03 and γ_2 = 3.12 ± 0.03, and the second knee γ_3 = 2.92 ± 0.03 and γ_4 = 3.34 ± 0.04.

In Fig. 3b comparison with other experiments: TALE [18] TA BR / LR [19], KASCADE-Grande [8] and Tunka [9]. One can see a good agreement of the spectra in the energy range 10^{16}-10^{18} eV. There is also a break in the spectrum at $\sim 10^{17}$ eV in other experiments as well. The

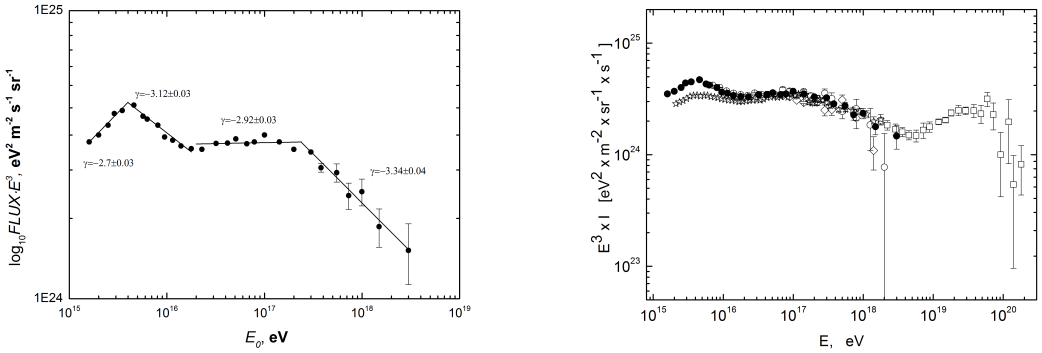

a) b)

Figure 3: A spectrum cosmic ray in the region 10^{16}-10^{18} eV by Yakutsk data (a) and comparison with other experiments (b).

spread in the spectrum is partly due to the different methods of estimating the energy at each of the EAS arrays and to some extent by the different effective thresholds of the arrays themselves.

6. Conclusion

For 20 years of continuous observations at the Yakutsk array, a large data of Cherenkov light in the energy region of 10^{16}-10^{18} eV was collected. This allowed us to obtain the following results: the air shower energy was estimated by the energy balance method of all shower particles and the spectrum of cosmic rays in the energy range 10^{16}-10^{18} eV is obtained. The spectrum has irregularity at the energy of $\sim 10^{17}$ eV. The slope of the spectrum changes from γ_3 = -2.92 to γ_4 = -3.34, everything indicates that at the energy of $\sim 10^{17}$ eV, the break is associated with astrophysical processes in our galaxy, as well as with extragalactic processes. The "second knee" phenomenon can be explained as transition from galactic to extragalactic cosmic rays.

Acknowledgement

The reported study was funded by RFBR according to the research project 16-29-13019.

References

[1] O. Adriani et al., Science **332**, no. 6025, 69-72 (2011).

[2] M. Aguilar et al., Phys. Rev. Lett. **114**, 171103 (2015).

[3] D.M. Green and E.A. Hays, Proc. of Sci. **301**, 159 (2018).

[4] A.D. Panov et al., Bull. of the RAoS: Physics, **73**, 564 (2009).

[5] E.S. Seo et al., Adv. Space Res. **42**, 1656 (2008).

[6] A. Aab et al., NIM A, **798**, 172-213 (2015).

[7] T. Abu-Zayyad et al., NIM A **689**, 87-97 (2012).

[8] W.D. Apel et al., Astropart. Phys. **36**, 183 (2012).

[9] V.V. Prosin et al. NIM A, **756**, 94 (2014).

[10] S. Knurenko, V. Kolosov and Z. Petrov. Proc. 27th ICRC (Hamburg) 1, 157-160 (2001)

[11] S. Knurenko et al. Sci. and Edu. **4**, 46-50 (1998)

[12] Y. Egorov, Z. Petrov and S. Knurenko, Proc. of Sci. **301**, 462 (2018).

[13] S.P. Knurenko et al. Proc. SPIE **6522**, 65221U (2006).

[14] S.P. Knurenko and I. Petrov, Proc. SPIE **9292**, 92925B (2014).

[15] S.P. Knurenko and I.S. Petrov, Proc. SPIE, **10466**, 1046659 (2017).

[16] S.P. Knurenko et al., JETP Lett. **83**, 473 (2006).

[17] S.S. Ostapchenko, Phys. Rev. D **74** 014026 (2006).

[18] R.U. Abbasi et al. ApJ, **865**, 74 (2018).

[19] R.U. Abbasi, et al., Astroparticle Physics **80**, 131-140 (2016).